Agricultural and Forest Meteorology 220 (2016) 38–49

Contents lists available at ScienceDirect

Agricultural and Forest Meteorology

journal homepage: www.elsevier.com/locate/agrformet

Evaluating atmospheric CO_2 effects on gross primary productivity and net ecosystem exchanges of terrestrial ecosystems in the conterminous United States using the AmeriFlux data and an artificial neural network approach

Shaoqing Liu[a], Qianlai Zhuang[a,b,*], Yujie He[a], Asko Noormets[c], Jiquan Chen[d], Lianhong Gu[e]

[a] Department of Earth, Atmospheric, and Planetary Sciences, Purdue University, West Lafayette, IN 47907, United States
[b] Department of Agronomy, Purdue University, West Lafayette, IN 47907, United States
[c] Department of Forestry and Environmental Resources and Southern Global Change Program, North Carolina State University, Raleigh, NC 27695, United States
[d] CGCEO/Geography, Michigan State University, East Lansing, MI 48824, United States
[e] Environmental Sciences Division, Oak Ridge National Laboratory, Oak Ridge, TN 37831, United States

ARTICLE INFO

Article history:
Received 18 March 2015
Received in revised form 5 January 2016
Accepted 8 January 2016
Available online 21 January 2016

Keywords:
Gross primary production
Net ecosystem change
Eddy flux tower
CO_2
Artificial neural network

ABSTRACT

Quantitative understanding of regional gross primary productivity (GPP) and net ecosystem exchanges (NEE) and their responses to environmental changes are critical to quantifying the feedbacks of ecosystems to the global climate system. Numerous studies have used the eddy flux data to upscale the eddy covariance derived carbon fluxes from stand scales to regional and global scales. However, few studies incorporated atmospheric carbon dioxide (CO_2) concentrations into those extrapolations. Here, we consider the effect of atmospheric CO_2 using an artificial neural network (ANN) approach to upscale the AmeriFlux tower of NEE and the derived GPP to the conterminous United States. Two ANN models incorporating remote sensing variables at an 8-day time step were developed. One included CO_2 as an explanatory variable and the other did not. The models were first trained, validated using eddy flux data, and then extrapolated to the region at a $0.05^o \times 0.05^o$ (latitude × longitude) resolution from 2001 to 2006. We found that both models performed well in simulating site-level carbon fluxes. The spatially-averaged annual GPP with and without considering the atmospheric CO_2 were 789 and 788 g C m^{-2} yr^{-1}, respectively (for NEE, the values were −112 and −109 g C m^{-2} yr^{-1}, respectively). Model predictions were comparable with previous published results and MODIS GPP products. However, the difference in GPP between the two models exhibited a great spatial and seasonal variability, with an annual difference of 200 g C m^{-2} yr^{-1}. Further analysis suggested that air temperature played an important role in determining the atmospheric CO_2 effects on carbon fluxes. In addition, the simulation that did not consider atmospheric CO_2 failed to detect ecosystem responses to droughts in part of the US in 2006. The study suggests that the spatially and temporally varied atmospheric CO_2 concentrations should be factored into carbon quantification when scaling eddy flux data to a region.

1. Introduction

Net ecosystem carbon exchange (NEE) and gross primary productivity (GPP) are two major fluxes involved in the ecosystem biogeochemical carbon process. Quantification of GPP and NEE and their responses to environmental changes would improve our understanding of the ecosystem carbon cycling and its feedbacks to the global climate system. At present, GPP and NEE at regional scales are often quantified using atmosphere inverse models (e.g. Prince and Goward, 1995), process-based biogeochemical models (e.g. White et al., 2000), and satellite remote sensing approaches (e.g. Running et al., 2000). The estimation of NEE based on the inverse models is limited by the sparseness of the carbon dioxide (CO_2) observation network (Tans et al., 1990); and this approach cannot differentiate the carbon source/sink contributions of each

* Corresponding author at: Purdue University, CIVIL 550 Stadium Mall Drive, West Lafayette, IN 47907, United States. Tel.: +1 7654949610.
E-mail address: qzhuang@purdue.edu (Q. Zhuang).

http://dx.doi.org/10.1016/j.agrformet.2016.01.007
0168-1923/

ecosystem (Janssens et al., 2003). Process-based models generally first derive the GPP and ecosystem respiration, which are modeled as a function of physical and biological variables and thus can be applied at regional and global scales. However, large uncertainty still exists in current quantification due to complex model structure, uncertain parameters, and model input (Chen et al., 2011). Satellite remote sensing approaches have advantages in GPP quantification that is based on a near real-time dataset, instead of broadly parameterized ecosystem models. However, they are highly dependent on the accuracy of the model algorithms and the quality of satellite imageries (Baldocchi et al., 2001).

The eddy covariance technique provides direct measurement of net carbon and water fluxes between vegetation and the atmosphere (Baldocchi et al., 1988; Foken and Wichura, 1996; Aubinet et al., 1999). At present, over 500 flux tower sites have been operated to measure the exchanges of carbon fluxes continuously over a broad range of climate and biome types (FLUXNET http://daac.ornl.gov/FLUXNET/fluxnet.shtml). These towers also provide calibrated, validated NEE data and the derived GPP product. To date, numerous studies have been conducted using those flux data to explore the GPP and NEE temporal or spatial variation and their controlling factors in terrestrial ecosystems (Valentini et al., 2000; Law et al., 2002; Baldocchi, 2008; Hirata et al., 2008; Kato and Tang, 2008; Lund et al., 2010; Bracho et al., 2012). Eddy flux data have also been widely used for model calibration (Baldocchi, 1997; Hanan et al., 2002; Reichstein et al., 2002; Hanson et al., 2004) and to upscale from stands to regional levels. The upscaling exercises generally employ the machine learning algorithm that uses meteorological data, vegetation properties, and remote sensing products, which have been conducted for Asia (Zhu et al., 2014; Fu et al., 2014), Europe (Jung et al., 2008; Vetter et al., 2008), the US (Yang et al., 2007; Xiao et al., 2008; Xiao et al., 2010) and even at global scales (Beer et al., 2010; Yuan et al., 2010).

However, few studies have incorporated the atmospheric CO_2 concentrations into regional GPP and NEE extrapolations when using eddy flux tower data. Increasing CO_2, which is mainly due to the burning of fossil fuels and, to a much lesser extent, land-cover change (Keeling et al., 1995; Hartmann et al., 2013), will have substantial direct and indirect effects on the carbon budget (Canadell et al., 2007). Numerous studies have been conducted to understand how plants and ecosystems will respond to elevated CO_2 (Ainsworth and Long, 2005). The large-scale free-air CO_2 enrichment experiment (FACE) showed that increasing CO_2 would reduce the stomatal conductance (Curtis and Wang, 1998; Medlyn et al., 2001; Ainsworth and Rogers, 2007) over a short time period, resulting in decreased transpiration, enhanced water-use efficiency (Conley et al., 2001; Wall et al., 2001) and increased soil moisture (Bunce, 2004). In addition, stimulated photosynthesis (e.g. Li et al., 2014) would increase the above and below-ground biomass production (Piao et al., 2006; Los, 2013; Wan et al., 2007; Deng et al., 2010) and hence accelerate the CO_2 loss from heterotrophic respiration (Luo et al., 1996). Generally, long-lived plant biomass (trees) is more responsive to increasing CO_2 than herbaceous species (Ainsworth and Long, 2005). However, increased plant production with high carbon (C) to nitrogen (N) ratio under elevated CO_2 results in low quality litter input and slows the soil N mineralization, thus triggering the negative feedback to plant biomass over time (Oren et al., 2001; Gill et al., 2002; Luo et al., 2004) if there is no extra nitrogen input. This conceptual framework about progressive N limitation is more obvious in long-lived plants (trees) (Luo et al., 2004) and has been supported by few experiments (Oren et al., 2001; Norby et al., 2010). In addition, the climate drivers and their interaction with soil resources (Reich et al., 2014) would also constrain the ecosystem response to CO_2 fertilization. For example, increasing N mineralization due to warming temperature would further promote plant growth (Peltola et al., 2002; Dijkstra et al., 2010) whereas the drought stress may diminish this positive effect under elevated CO_2 condition (Dermody et al., 2007; Larsen et al., 2011). Moreover, altered water, energy balance (Drake et al., 1997; Keenan et al., 2013), and vegetation physiology due to increasing CO_2 would in turn affect the carbon cycling. Therefore, incorporating atmospheric CO_2 concentrations into the regional GPP and NEE estimation should be a research priority. In addition, previous upscaling flux studies that exclude the atmospheric CO_2 concentration assume that CO_2 variations were spatially and temporally uniform in a region. Although atmospheric CO_2 is generally well-mixed globally since it is chemically inert (Eby et al., 2009), it actually exhibits a large seasonal and spatial variability at the regional scale (Miles et al., 2012). The seasonal and spatial characteristics have previously been reported at site and regional levels (Davis et al., 2003; Haszpra et al., 2008; Miles et al., 2012). For example, the summer measurement of the atmospheric boundary layer CO_2 mole fraction from a nine-tower regional network deployed during the North American Carbon Program's Mid-Continent Intensive (MCI) during 2007 to 2009 shows that the seasonal CO_2 amplitude is five times larger than the tropospheric background and the spatial gradient across the region is four times the inter-hemispheric gradient (Miles et al., 2012).

In this study, we used an artificial neural network (ANN) approach to upscale the AmeriFlux tower derived GPP and NEE to the conterminous US from 2001 to 2006 by considering the atmospheric CO_2 concentrations as an independent factor. We developed two sets of ANN models linking GPP and NEE and remote sensing variables for each vegetation type: the first considered the atmospheric CO_2 concentration effects (CO_2 incorporated simulation, S0) and the other did not (non-CO_2 incorporated simulation, S1). After the training and validation procedure, we then used the two models to extrapolate GPP and NEE to the conterminous US. We hypothesized that: (1) both models would capture the GPP and NEE variation at the calibration stage; (2) the two simulations would exhibit spatiotemporal differences which associate with climate drivers; and (3) ecosystems with high productivity (e.g., forest, cropland) would show greater differences between the two simulations.

2. Method

2.1. Overview

From the AmeriFlux network, we selected the key ecosystem types in the conterminous US including: evergreen forest, deciduous forest, grassland, mixed forest, savannas, shrubland, and cropland. Day land surface temperature (D_LST) and night land surface temperature (N_LST), leaf area index (LAI), fraction of absorbed photosynthetically active radiation (fPAR), normalized difference vegetation index (NDVI), enhanced vegetation index (EVI), CO_2 measurement and derived GPP and NEE from the eddy flux towers were organized into an 8-day time step. To explore the atmospheric CO_2 concentrations' effect on the GPP and NEE, we constructed two sets of ANN models for each vegetation type: one incorporated CO_2(S0) in addition to D_LST, N_LST, LAI, fPAR, NDVI and EVI; and the second did not incorporate with CO_2 (S1) with the same explanatory variables in S0. After the training and validation of the two sets of ANN models, the regional estimation of GPP and NEE was driven by the explanatory variables at a spatial resolution of $0.05^\circ \times 0.05^\circ$ on an 8-day time step. The difference between S0 and S1 was then analyzed, considering the controls of environmental variables.

Table 1
Ameriflux Sites used in ANN models.

Site name	Site ID	Vegetation type	Data range
ARM SGP Control	US-Arc	Grasslands	2005–2006
ARM SGP Main	US-ARM	Cropland	2003–2006
Bartlett Experimental Forest	US-Bar	Deciduous broadleaf forest	2004–2005
Blodgett Forest	US-Blo	Evergreen needleleaf forest	2000–2006
Duke Forest Hardwoods	US-Dk2	Mixed Forest	2001–2005
Duke Forest Loblolly Pine	US-Dk3	Evergreen needleleaf forest	2001–2005
Fermi Agricultural	US-IB1	Cropland	2005–2006
Fermi Prairie	US-IB2	Grasslands	2004–2006
Fort Dix	US-Dix	Mixed Forest	2005–2006
Freeman Ranch Mesquite Juniper	US-FR2	Woody savannas	2004–2006
Harvard Forest	US-Ha1	Deciduous broadleaf forest	2000–2006
Harvard Forest Hemlock	US-Ha2	Evergreen needleleaf forest	2004
Howland Forest Main	US-Ho1	Evergreen needleleaf forest	2000–2004
Kendall Grassland	US-Wkg	Grasslands	2004–2006
Kennedy Space Center Scrub Oak	US-KS2	Shrubland	2000–2006
Mead Rainfed	US-Ne3	Cropland	2001–2005
Mead Irrigated	US-Ne1	Cropland	2001–2005
Mead Irrigated Rotation	US-Ne2	Cropland	2001–2005
Metolius Intermediate Pine	Us-Me2	Evergreen needleleaf forest	2003,2005
Metolius Second Young Pine	Us-Me3	Evergreen needleleaf forest	2004–2005
Morgan Monroe State Forest	US-MMS	Deciduous broadleaf forest	2000–2005
Lost Creek	US-Los	Shrubland	2001–2005
Missouri Ozark	US-MOz	Deciduous broadleaf forest	2004–2006
North Carolina Loblolly Pine	US-NC2	Evergreen needleleaf forest	2005–2006
Ohio Oak Openings	US_Oho	Deciduous broadleaf forest	2004–2005
Santa Rita Mesquite Savanna	US-SRM	Woody savannas	2004–2006
Sky Oak Old	US-SO2	Shrubland	2005–2006
Sky Oak Young	US-SO3	Shrubland	2005–2006
Sylvania Wilderness	US-Syv	Mixed Forest	2002–2006
Tonzi Ranch	US-Ton	Woody savannas	2001–2006
Univ of Mich Biological Station	USMS	Mixed Forest	2000–2003
Vaira Ranch	US-Var	Grasslands	2001–2006
Willow Creek	US-Wcr	Deciduous broadleaf forest	2000–2006
Wind River Field Station	US-Wrc	Evergreen needleleaf forest	2000–2004
Wisconsin Intermediate Hardwoods	US_Wi1	Deciduous broadleaf forest	2003
Wisconsin Mature Red Pine	US-Wi4	Evergreen needleleaf forest	2002–2005

2.2. Explanatory variables

NEE is the difference between photosynthesis and ecosystem respiration, which is influenced by a variety of physical, physiological, hydrological, and atmospheric variables. As for the plant photosynthesis, current ecosystem models have incorporated various mechanisms related to these factors to simulate GPP, such as the bio-chemical model (e.g. Farquhar et al., 1980), light use efficiency equation (e.g. Running et al., 2000), and the semi-empirical relationship (e.g. Raich et al., 1991). Ecosystem respiration (Re) includes autotrophic (Ra) and heterotrophic respiration (Rh). Ra is generally modeled as a function of temperature and plant biomass, while Rh is empirically modeled as a function of soil temperature, moisture, and soil organic carbon stocks. Many of these factors influencing GPP and NEE can be assessed by satellite remote sensing products. NDVI is closely correlated to the photosynthetic activity, vegetation biomass, and fractional vegetation cover, which have been widely used in production efficiency models. We also incorporated the EVI to improve the ANNs performance due to the several limitations of normalized difference vegetation index (NDVI), including the saturation in a multilayer closed canopy and sensitivity to atmosphere aerosols and soil background. The LST derived from the Moderate Resolution Imaging Spectroradiometer (MODIS) corresponds the surface soil temperature, which is known to strongly control the Re as both Ra and Rh. Previous studies demonstrated that satellite-derived LST was strongly correlated with Re, especially in dense-vegetated ecosystems (Rahman et al., 2005). The estimation of LAI and fPAR, characterizing the vegetation canopy function and energy absorption capacity, are key parameters in most biogeochemical models due to the high correlation with GPP. Taken together, we selected LST, NDVI, EVI, fPAR, and LAI as explanatory variables to account for the GPP and NEE variation.

2.3. Data organization

We organized AmeriFlux site-level data of carbon flux and meteorology, MODIS land-cover, spatially and seasonally explicit CO_2, and the remote sensing products derived from MODIS. The AmeriFlux network coordinates regional analyses of observations from eddy covariance flux towers across the US. The Level-3 and Level-4 data for 36 AmeriFlux sites over the period 2000–2006 that contained CO_2 measurements were ultimately organized (Table 1 & Fig. 1). In the Level-3 product, the half-hourly CO_2 was aggregated into 8-day time step values. The Level-4 product consists of two types of GPP and NEE data: standardized (GPP_st and NEE_st) and original (GPP_or and NEE_or). Here, we used the same method in Xiao et al. (2010) to select the type of GPP and NEE product. Explanatory variables, GPP and NEE values derived from the selected sites were organized to develop the ANN models for each ecosystem type.

We used the following four MODIS data products (Collection 4), including daytime and nighttime LST (MOD11A2; Wan et al., 2002), EVI (MOD13A1; Huete et al., 2002), and LAI/fPAR (MOD15A2; Myneni et al., 2002). EVI is at a spatial resolution of 500 m × 500 m, while LAI, fPAR, and LAI are at spatial resolutions of 1 km × 1 km. These MODIS data were resampled to the same resolution of 0.05° × 0.05° (longitude × latitude). The explicitly spatial and seasonal CO_2 data was obtained from the National Oceanic and Atmospheric Administration (NOAA) gridded CO_2 product (ftp://aftp.cmdl.noaa.gov/products/carbontracker/co2/). The product is based on global CO_2 observation network data, employing

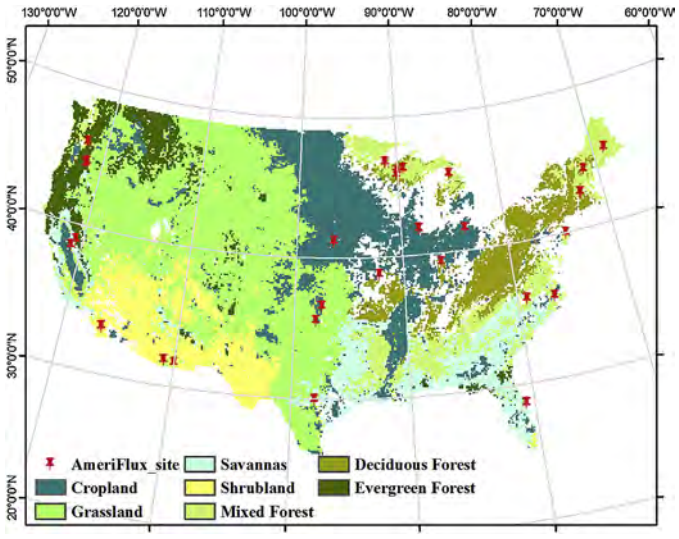

Fig. 1. Selected AmeriFlux tower sites in this study.

a novel ensemble assimilation method to accurately model atmospheric CO_2 mole fractions (Peters et al., 2007). Land cover was obtained from the MODIS product Land Cover Types Yearly L3 Global 0.05 Deg CMG (MOD12C1) (Year 2005) from the NASA Goddard Space Flight Center website (http://modis-land.gsfc.nasa.gov). The classification of the International Geosphere and Biosphere (IGBP) land-cover classification system was used to reclassify the land-cover map of the conterminous United States into seven major vegetation types in the ANN model. To be more specific, the evergreen needleaf forest and evergreen broadleaf forest were combined into evergreen forest (same for deciduous forest); and closed shrubland and open shrubland were merged into shrubland. Therefore, the model calibration and simulation were based on the seven vegetation types: evergreen forest, deciduous forest, grassland, mixed forest, savannas, shrubland, and cropland.

2.4. Neural network development

We used a General Regression Neural Network (GRNN) algorithm (Specht, 1991) to represent the input-output relationship between the independent variables and dependent variables. The GRNN scheme can model the nonlinear system without specifying the algebraic relationship or internal mechanism. With the advantage of a fast-learning speed and good convergence with a large number of training datasets, GRNN can be a useful tool to estimate GPP and NEE based on the explanatory environmental variables. The training data set, including input and output values of measurements, is fed into the multilayer neural network. The network is trained to obtain a set of optimized interconnected network weights, which are used to produce the most probable value for the outputs. More details about the GRNN algorithm and optimization procedure are provided in the supplementary information (GRNN algorithm and Fig. S1). To develop the GRNN model for each ecosystem type, we first randomly divided each dataset into two sets: a training set (75% of whole data for each vegetation type) used to construct the GRNN model and a testing set (25% of whole data for each vegetation type) used to evaluate the performance of constructed GRNN. MATLAB codes were used for developing the model (The MathWorks Inc., Natick, MA, USA).

The uncertainty of GRNN model prediction is mainly from three sources: input variables, ANN model structure, and model parameters. Here we focused on the uncertainties associated with the model structure because we do not have sufficient knowledge about the uncertainty of input variables. We used the "delete-one" method (Zhuang et al., 2012) through developing a number of alternative ANN models to quantify the uncertainty of GPP and NEE due to uncertain model structures. To be more specific, we randomly selected 75% of the observed data for each ecosystem type to develop a new ANN model. The new model was then scaled up to obtain the new GPP and NEE estimation at the regional scale. The process was repeated for 100 times in S0 and S1 for each ecosystem type, respectively. The averaged GPP and NEE of all estimations were used to analyze the differences among simulations. The 95% confidence intervals were considered to be the range of model uncertainty to define the upper and lower bounds of the GPP and NEE estimation.

3. Results

3.1. Annual GPP and NEE and spatial difference

The simulated GPP, NEE with the two sets of ANN models were both close to the observed GPP and NEE for each ecosystem type (Fig. S2). We applied the two sets of models to calculate the annual averaged GPP and NEE of terrestrial ecosystems for the conterminous US at an 8-day time step from 2001 to 2006 (Fig. 2a and c). Both models showed a high spatial variability with a clear gradient from west to east. The Gulf Coast and parts of the Southeastern US were the most productive regions, with GPP greater than 2000 g C m^{-2} yr^{-1}. Most parts of the Southeast and coastal Pacific Northwest also possessed high GPP (1250–1500 g C m^{-2} yr^{-1}). The Northeast had intermediate GPP (500–1000 g C m^{-2} yr^{-1}), where was mainly dominated by deciduous forest. The Midwest, Southwest and Rocky Mountain areas generally had relatively low GPP (<500 g C m^{-2} yr^{-1}). As for spatial patterns of NEE, the greatest net carbon uptake took place in the Gulf Coast and Mideast, with the annual averaged value of −800 g C m^{-2} yr^{-1}. By contrast, the Rocky Mountain area had the highest contribution to carbon release across the conterminous US. The uncertainty analysis based on the 100 ANN models (Fig. S3) demonstrated that our ANNs models predicted GPP and NEE with a small uncertainty across the whole ecosystem type. Overall, both simulations indicated that the East and Pacific Northwest showed high ecosystem productivity, acting as a carbon sink, while the Rocky Mountain region had the lowest GPP value and acted as a carbon source to the atmosphere.

The two simulations however, diverged in regions including the Pacific Northwest coast, Gulf coast and most parts of Southeast dominated by evergreen forests, savannas and mixed forest (Fig. 2b and d). S0 exhibited lower GPP (−200 to −100 g C m^{-2} yr^{-1}) and more positive NEE (100–250 g C m^{-2} yr^{-1}) value in most Southeastern US than that of S1 (Fig. 2b). In contrast, west North Central region had higher GPP (100–200 g C m^{-2} yr^{-1}) and more negative NEE (−150 to −50 g C m^{-2} yr^{-1}) in S0. From the vegetation perspective, the relative difference of GPP and NEE in the mixed forest and cropland showed a spatial variability. Specifically, the lower estimation of GPP in mixed forests and cropland was mainly found in the Southeast and east of South Central, while a higher GPP was observed in the North Central in S0. These patterns were similar to the NEE estimation (Fig. 2d).

3.2. Seasonal GPP and NEE difference

Our 8-day GPP and NEE estimation based on the two ANN models both captured the seasonal flux variability in the conterminous US (Fig. 3 and Fig. S4). Take the GPP seasonal pattern, for example; in spring (March to May), the Gulf Coast and the Pacific Northwest region began to assimilate carbon at 100–200 g C m^{-2} yr^{-1}, followed by the Southeast and the South Central. In contrast, most of the Northeast and Rocky Mountain area possessed a low GPP due to the relatively cold weather or late leaf-out. Plants reached

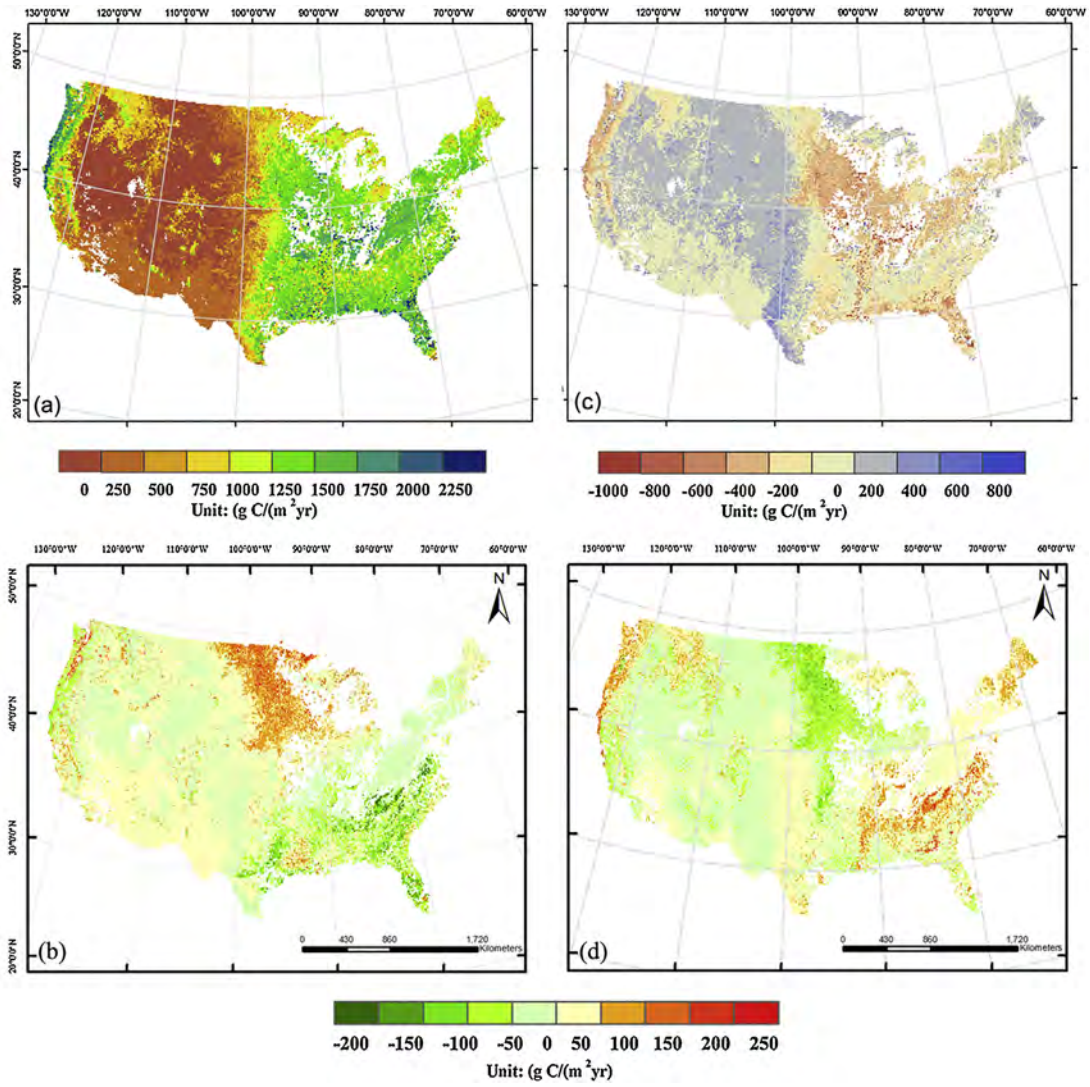

Fig. 2. Annual averaged GPP (a) and NEE (c) in S0 and their differences (GPP (b), NEE (d)) between S0 and S1across the conterminous US scale from 2001 to 2006 (Unit: g C/(yr m^2)). The difference is calculated as S0 minus S1. S0 and S1 are the simulations with and without considering the atmospheric CO_2 concentration, respectively.

the greatest productivity in summer (June–August) with the highest GPP of 300–400 g C m^{-2} yr^{-1} in the Northeast regions. From fall (September–November) to winter (December–February), GPP decreased drastically to either a low level (50–100 g C m^{-2} yr^{-1}) in the Gulf Coast, Pacific Northwest and South Central or nearly zero in most parts of Rocky Mountains throughout the US.

The obvious difference between seasonal GPP and NEE generally occurred in mixed forests and croplands (Fig. 4 and Fig. S5). In the early spring (March–April), the mixed forest in the Southeast began to exhibit lower GPP and more positive NEE in S0, and this difference was much stronger from late spring (May) to early fall (September). However, for the mixed forest in North Central and the Northeast, the difference only took place in June, July, and August. And this was similar for cropland in North Central, which only showed higher GPP and more negative NEE in these three months. No obvious difference was observed between the two simulations in winter.

3.3. GPP and NEE response to CO_2concentrationsunder drought condition

Annual GPP and NEE both exhibited positive and negative anomalies each year. The anomalies could have been due to climate variability, disturbances, management practices, or model errors. The severe drought affected over 50% of the country, including the Southwest, the Great Plains, the Gulf Coast, the coastal Southeast, and particularly Texas and Oklahoma. Therefore, we evaluated the GPP and NEE response to the drought condition in 2006. Both models showed negative anomalies in most regions, like the Great Plains (Fig. 5). However, as for the Southeast and parts of North Central, the S0 exhibited the negative GPP and positive NEE anomalies when compared with S1. According to the US Drought Monitor (http://www.drought.unl.edu) and the PRISM database, these regions showed around 250 mm less precipitation in 2006. Without considering the CO_2 effect in upscaling GPP and NEE, the S1 failed to show the ecosystem response to severe drought condition.

4. Discussion

4.1. Comparison of S0 and S1 with other studies

Our estimation of GPP and NEE and their spatial variations agreed well with previous published results. For example, Xiao et al. (2010) estimated that the spatially averaged GPP across the conterminous US scaled at 907 g C m^{-2} yr^{-1}. Our simulation showed that the Gulf Coast and parts of the Southeast were the

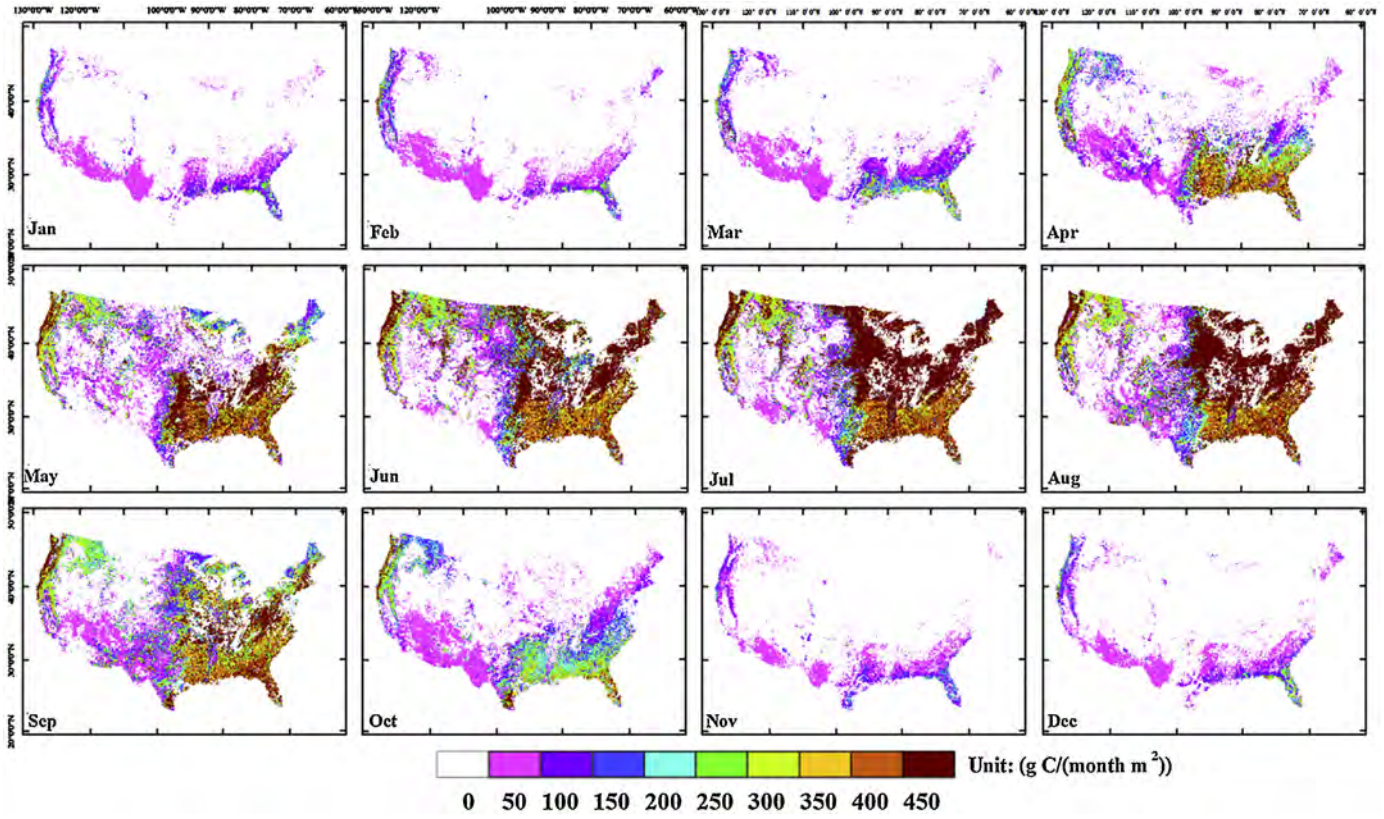

Fig. 3. Averaged monthly GPP (g C/(month m^2)) for the conterminous U.S. from January through December from 2001 to 2006 in S0. S0 is the simulation with considering the atmospheric CO_2 concentration.

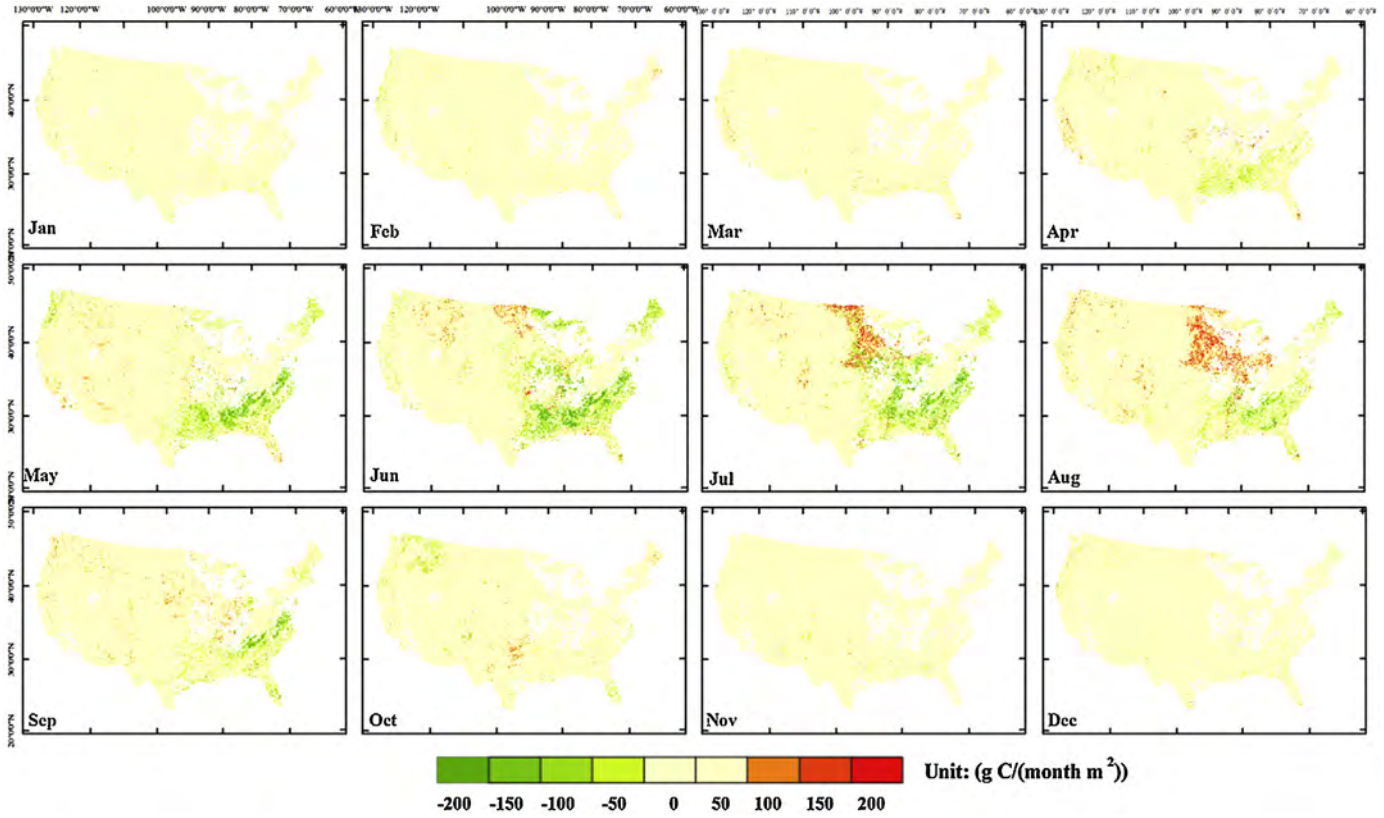

Fig. 4. Averaged monthly GPP difference (g C/(month m^2)) between S0 and S1 for the conterminous U.S. from January through December from 2001 to 2006. The difference is calculated as S0 minus S1.S0 and S1 are the simulations with and without considering the atmospheric CO_2 concentration, respectively.

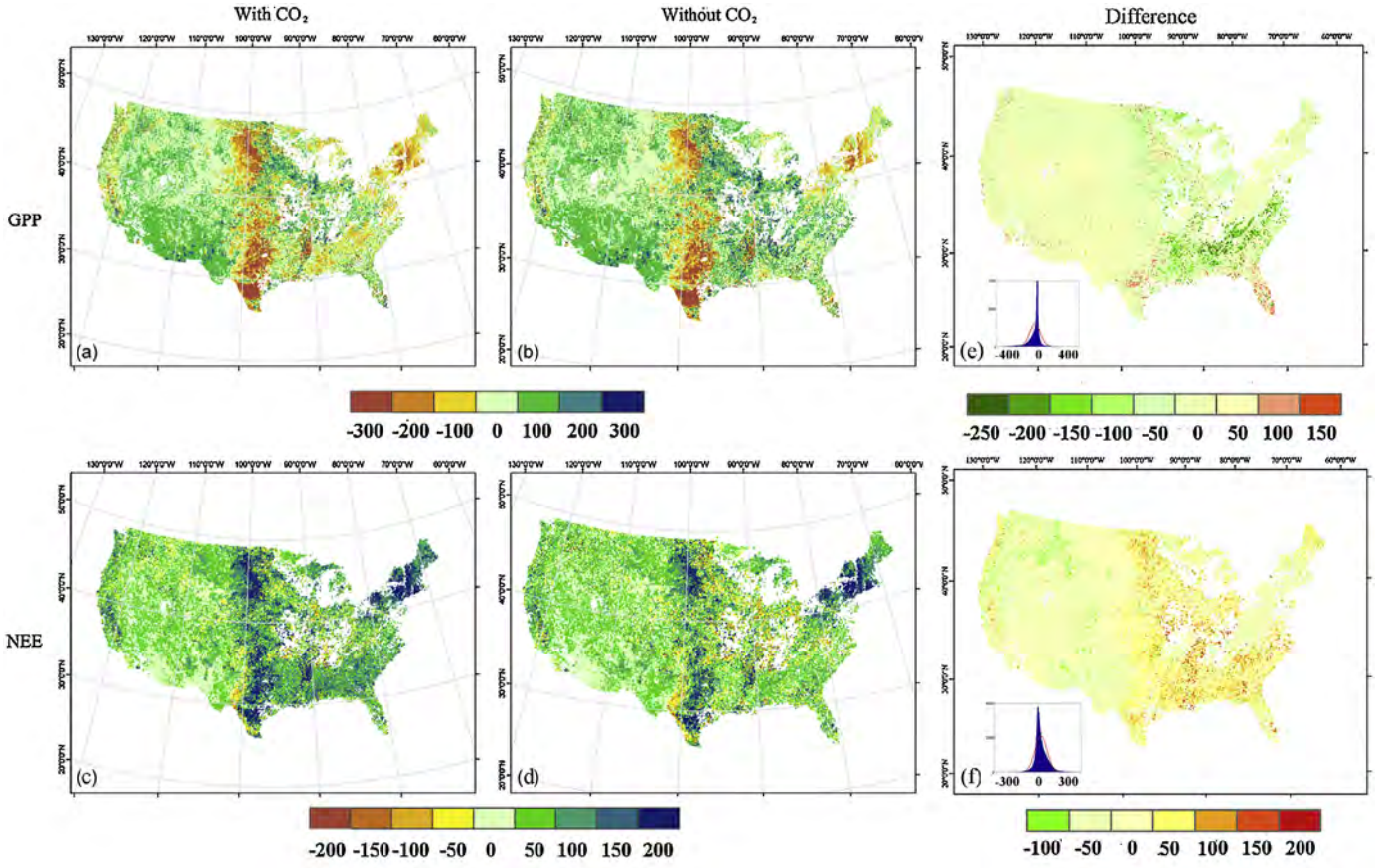

Fig. 5. Annual GPP (a and b), NEE (c and d), and anomalies in S0 and S1 for the conterminous U.S. at 2006. The anomalies of annual GPP and NEE at 2006 were relative to the 6-year average value. The anomalies difference (e and f) is calculated as S0 minus S1.S0 and S1 are the simulations with and without considering the atmospheric CO_2 concentration, respectively.

most productive regions, with GPP greater than 2000 g C m^{-2} yr^{-1}, and was consistent with previous studies (Yang et al., 2007; Xiao et al., 2010; Chen et al., 2011). The total gross carbon uptake estimated in both models was 4.00 and 3.95 Pg yr^{-1}, respectively, and was lower than the results of Xiao et al. (2010) because we did not reclassify the cropland/natural vegetation mosaic in MODIS land cover product as cropland ecosystems. In addition, the estimation of GPP (1250–1500 g C m^{-2} yr^{-1}) in the Southeast was much lower than Xiao's et al. (2010) prediction (>2250 g C m^{-2} yr^{-1}), but was comparable with Chen's et al. (2011) study and the MODIS GPP product (Running et al., 2004). The spatially averaged GPP in two simulations generally agreed well with MODIS GPP (Fig. S6) ($R^2 > 0.8$). However, MODIS GPP (<800 g C m^{-2} yr^{-1}) was markedly underestimated in cropland compared with our models (>1000 g C m^{-2} yr^{-1}). This large difference may be attributable to that MODIS GPP, which was based on the light use efficiency algorithm while ANN was based on the site-level flux tower data. The key parameter, the maximum light use efficiency in the MODIS GPP algorithm, was always underestimated and thus led to lower estimation in high productivity areas (Turner et al., 2006; Xiao et al., 2010). Recently, Madani et al. (2014) used eddy flux carbon data to show that the optimum light use efficiency in cropland was twice as much as that in the MODIS GPP algorithm.

4.2. Climate controls on the CO_2 effects on GPP and NEE

Previous studies have evaluated the interactions between elevated CO_2 and other environmental variables, such as increasing temperature (Peltola et al., 2002; Tingey et al., 2003; Hovenden et al., 2008; Dijkstra et al., 2010) and hydrological conditions (Morgan et al., 2004; Nowak et al., 2004). Increasing CO_2 with enhanced N mineralization at higher temperatures may further promote plant growth (Kirschbaum et al., 1994), whereas the positive effect may be ameliorated in a reduced precipitation environment due to the slow turnover rate of N belowground (Emmett et al., 2004; Sowerby et al., 2008). The seasonal GPP and NEE difference in our simulations also indicated there were interactions between CO_2 effect and climate drivers. Obvious GPP and NEE difference can only been observed from late spring to summer in the Northern forest ecosystem (Fig. 4 and Fig. S5), suggesting that the temperature controlling the plant phenology may play a key role in CO_2 effects on the carbon fluxes. In addition, evergreen forest in Pacific Northwest exhibited lower GPP in May and October (Fig. 4), indicating that drought or the soil water deficit (Law et al., 2000; Schwarz et al., 2004) may impact the CO_2 effects. The seasonal variation of NEE difference was slightly different from GPP (Fig. 4 and Fig. S5). NEE differences were shown earlier than GPP in spring, especially in the Northern forest. The enhanced heterotrophic respiration due to soil warming (Raich and Schlesinger, 1992; Lloyd and Taylor, 1994) may result in the asynchronicity of GPP and NEE's response to the atmospheric CO_2 effect.

We analyzed the causes for the spatial variability of GPP difference using annual averaged air temperature (T_a) and vapor pressure deficit (VPD) (Fig. 6). We obtained the Ta and VPD from North American Regional Reanalysis dataset (Mesinger et al., 2006). The atmosphericCO_2 concentration showed negative effect on the evergreen forest and the effect was more obvious under high temperature condition (>285 K). Both deciduous forest and shrubland

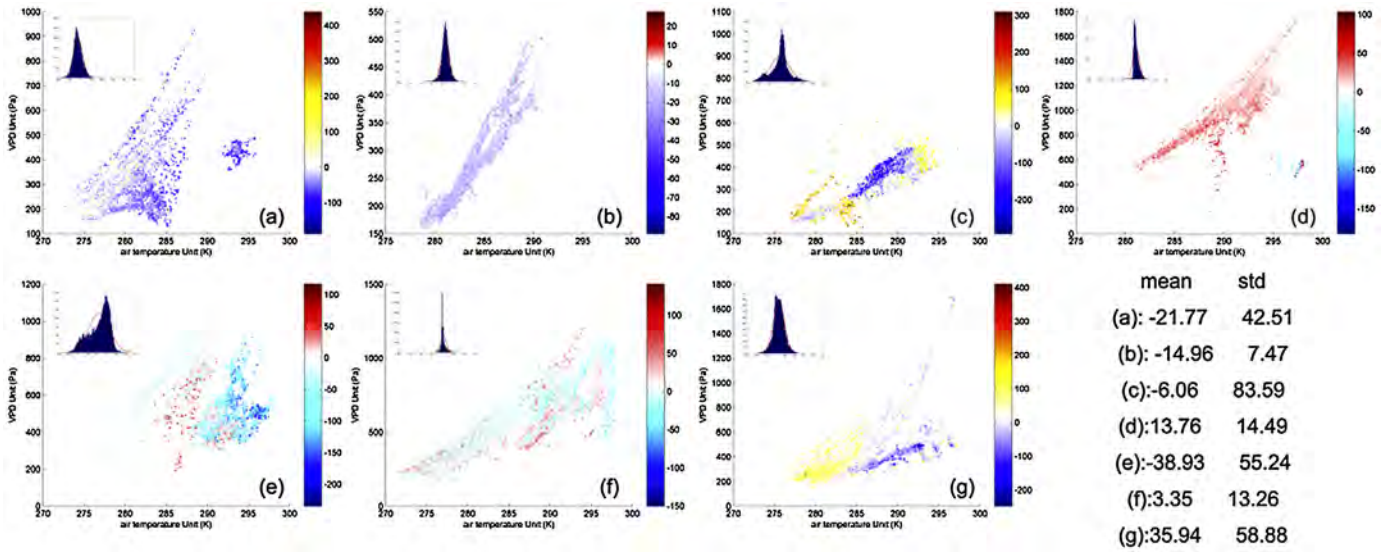

Fig. 6. Air temperature and VPD controls on the annual GPP difference (the difference is calculated as S0 minus S1) spatial variability for each vegetation type:(a) Evergreen forest; (b) Deciduous forest;(c) Mixed forest; (d) Shrubland; (e) Savannas; (f) Grassland; and (g) Cropland. The mean values and standard deviations of GPP difference in each vegetation types are presented. S0, and S1 are the simulations with and without considering the atmospheric CO_2 concentration, respectively.

did not show a obvious difference across the T_a and VPD ranges. However, for the mixed forests, the difference could be divided by the T_a value around 285 K. The GPP estimation in S0 was generally lower when T_a >285 K but higher when T_a < 285 K, when compared with S1. This was similar for the cropland; a lower GPP estimation occurred in S0 when T_a > 285 K and it had a higher estimation when T_a < 285 K. In addition, the negative effect was much stronger in lower VPD ranges (VPD < 600 Pa), indicating that the CO_2 had stronger effect in the humid area. As for the savannas, no obvious Ta threshold was observed and the negative effect generally located in the high Ta range. CO_2 concentration showed complex effect on grassland, but overall, had a small influence on GPP estimation. Fig. 5 also gave the statistical values (mean and standard deviation) of the GPP difference between the two simulations in each ecosystem type. Although the spatially averaged GPP difference was generally small (<50 g C m^{-2} yr^{-1}), the coefficient of variation (the ratio of standard variation to mean value) was great in mixed forest and evergreen forest, followed by cropland and savannas.

4.3. GPP and NEE response to atmospheric CO_2 under drought condition

Remote sensing has been widely used to monitor the spatial patterns of drought and its related changes in global ecosystems. Previous studies implemented the vegetation indices (NDVI, NDWI) from Advanced Very High Resolution Radiometer (AVHRR) (Tucker, 1979) and MODIS to detect drought conditions over the Great Plains in the US (Gu et al., 2007), East Asia (Song et al., 2004), and Amazonian forest (Anderson et al., 2010). Due to the lagged response of vegetation to the drought events, these vegetation indices were combined with land surface thermal infrared information to improve drought detection (Singh et al., 2003; Park et al., 2004; Wan et al., 2004; Son et al., 2012). In this study, the negative anomalies of GPP in the Southeast only occur in S0, although both simulations captured the vegetation response to drought events in 2006, especially in the low biomass ecosystem (grassland, shrubland), by exploring the vegetation indices and thermal information. The spatial pattern of GPP anomalies in S1 was similar with Xiao et al. (2010), which also incorporated MODIS products using the regression tree model. Park et al. (2004) demonstrated that soil water-holding capacity affected the drought detection when using MODIS vegetation indices and thermal information. Gu et al. (2008) also pointed out that the various correlations between MODIS, NDVI, NDWI and drought events were highly dependent on the vegetation structure and soil types. Drought stress with reduced soil moisture can constrain plant nutrient uptake by reducing nutrient supply through mineralization(Emmett et al., 2004; Sowerby et al., 2008; Larsen et al., 2011), also by reducing nutrient diffusion and mass flow in soils (Lambers et al., 2008). Therefore, the induced drought condition may potentially decouple the soil microbial carbon and soil CO_2 fluxes with canopy photosynthesis (Ruehr et al., 2009), increasing the residence of recent assimilated carbonate in vegetation (Deng et al., 1990; Li and Wang, 2003) and thus affecting the whole ecosystem carbon and nitrogen cycling. Some studies also pointed out the great contribution of drought to the surface CO_2 variability (Knorr et al., 2005; Keppel-Aleks et al., 2014). The climate of the Southeast is predicted to be warmer and drier in future (Dai, 2013). Therefore, incorporating the atmospheric CO_2 concentration into an upscaling practice using the flux site data should improve the qualification of GPP and NEE and strengthen our understanding of vegetation's response to environmental condition.

4.4. Implication of the CO_2 effect on GPP and NEE

Since atmospheric CO_2 is an important factor related to plant carbon assimilation and water balance, incorporating it is expected to improve our understanding on the ecosystems' response to environmental variables. However, previous studies concerning the degree of climate controls on the spatial and temporal patterns of the eddy covariance derived GPP and NEE (e.g. Yu et al., 2013) or upscale the site-level data to regional estimation (e.g. Xiao et al., 2010) always ignored the atmospheric CO_2 concentration. As our study statistically demonstrated above, including CO_2 as an explanatory variable in upscaling site-level eddy flux data to regional GPP and NEE made an obvious seasonal and spatial difference. Taking the North Central region of US as an example, our results demonstrated that GPP was about 200 g C m^{-2} yr^{-1} higher in S0 due to the overestimation in the growing season; this implied that larger GPP and NEE differences may occur between the two simulations when atmospheric CO_2 showed a greater variability during these periods. Furthermore, excluding the atmospheric CO_2

concentration, the regional GPP and NEE variation may be overly attributed to other climate variables.

Up to now, most of the regional and global estimations of terrestrial carbon uptake come from various ecosystem biogeochemistry models, which are mathematical representations of biophysical processes (Bonan, 2008). The model constrained with eddy flux towers observation would strengthen the understanding of ecosystem mechanisms. This data-assimilation method provides an alternative way to quantify regional carbon exchanges between the terrestrial biosphere and the atmosphere at regional and global scales (Xiao et al., 2012). Generally, flux measurements are used to calibrate the parameters in ecosystem models, and then the optimized parameters are extrapolated for the estimation over a region. In some process-based ecosystem models which use CO_2 data as an input to compute GPP, the carbon fluxes are routinely calibrated and simulated based on annual CO_2 time series (or to be more specific, the background CO_2 concentration) across a region or globe (Turner et al., 2003; Chen et al., 2011). However, although CO_2 is generally well-mixed globally since it is chemically inert (Eby et al., 2009), it may exhibit a large local variability at short time scales. A recent study by Keppel-Aleks et al. (2014) also underscored the need to consider the full spatial and temporal distribution of atmospheric CO_2 to accurately separate the climate events' (e.g., warming and drought) influence on carbon cycling. Thus, GPP and NEE estimation should be improved if spatially- and temporally-varied atmospheric CO_2 data are used.

4.5. Limitation

There are a number of limitations in our ANN estimations. First, the gridded CO_2 product was developed using a global inversion model, whose accuracy is highly dependent on the prior CO_2 fluxes (Masarie et al., 2011). In addition, inaccurate weather data in complex terrain also introduces errors by using the transport model (TM5) at coarse spatial resolutions (Geels et al., 2007). The uncertain CO_2 product may bias our GPP and NEE estimations. To assess the uncertainty of the NOAA CO_2 products, we did a comparison analysis between the 8-daily averaged NOAA gridded CO_2 values and the in-situ CO_2 observation in summer season at seven sites (Fig. S7). Generally, the extracted CO_2 seasonal variations from NOAA products were comparable with the CO_2 measurement at forests (Fig. S7a–S7c) and crop sites (Fig. S7g), with the differences ranging from 5 to 15 ppmv. The site-level sensitivity analysis (Fig. S8) showed that these CO_2 input data differences would change annual GPP by 8–50 g C (2–6% relative change) using ANN models. In particular, the GPP changes in the mixed forest and croplands were almost two times larger than in other ecosystems. Despite the uncertainty of the gridded CO_2 product, we used it to gain insight into the effects of CO_2 on regional GPP and NEE prediction when upscaling site-level data. High frequency, stable CO_2 measurements (Andrews et al., 2014) and high-density observation networks (Lauvaux et al., 2012) are needed to accurately quantify the atmospheric CO_2 effects on GPP.

Second, the selected AmeriFlux sites can contribute a large uncertainty to our model development, because ANN training and validating are highly associated with the eddy flux data. The representativeness of the AmeriFlux data is crucial to scaling up site-level measurement to large regions. In our study, the criterion to select sites is based on the available CO_2 measurement from 2000 to 2006. The representativeness of the flux sites is crucial to scaling up site-level measurement and to understand the carbon dynamics across large spatial scales and quantify uncertainty. Although the global sites well represent variations in climate and ecological regions (Reichstein et al., 2014), whether the major ecoregions from North America are well represented by the AmeriFlux network has not been examined (Hargrove et al., 2003). Using a cluster analysis with 25 climatic and physiological forcing variables based on 59 AmeriFlux sites, Hargrove et al. (2003) showed that the vast interior of the US was well-represented by the AmeriFlux network, but the Pacific Northwest, Southern, and Southwestern were under represented. In addition, the uncertain eddy flux data – due to system errors, random errors, site selection criteria (Loescher et al., 2006), and the gap-filling method (Moffat et al., 2007; Desai et al., 2008) – may affect the GPP and NEE uncertainty in the model parameterization and simulation.

Third, our approach has not considered other controlling factors on the carbon fluxes. The vegetation distribution was constant without any shifts or disturbances during the study period, which might have biased estimation. Lacking the effects of land-cover changes, natural disturbances (e.g., fire, hurricane, insect infestation), economic influences (e.g., harvest) and demographic factors (Lambin et al., 2003) would also introduce uncertainties to our quantifications. Especially in the US, about half of the forest area is disturbed each decade, including the timber harvesting and grazing (Birdsey and Lewis, 2003). The forest age reflects the past disturbance history. Use of the North American forest stand age database (Pan et al., 2011) derived from forest inventory, historical fire data, and remote sensing imagery could help reduce our quantification uncertainty (Deng et al., 2013; Xiao et al., 2014). For cropland, without considering the effects of crop rotation (such as from corn to soybeans) may also introduce uncertainty. Since C4 photosynthetic capacity is different from C3 plant, explicit C3 versus C4 plant distribution data shall also help reduce the uncertainty of carbon qualification. In addition, the MODIS ecosystem distribution is not consistent with flux tower footprints (Xiao et al., 2008) and can be significantly different from the towers' vegetation type. Recent studies by Melton and Arora (2013) showed that the plant function type variability within the one-grid scale is important in simulating ecosystem responses to changing climate and atmospheric CO_2 concentration.

Fourth, using only seven plant functional types (PFTs) derived from the MODIS land use product may also introduce uncertainties to the carbon flux quantification. In the simulations, we assumed that, at each PFT level, the response of carbon fluxes to environmental condition changes is same. The usefulness and accuracy of such assumption has been questioned by field ecologists and there is a significant overlap between PFTs (Reich et al., 2007). The PFT-level parameterization could be biased because it may not properly represent the functional and structural characteristics of the species within a region. The parameter values obtained at the PFT level led to diverse significant carbon dynamic quantifications (Alton, 2011; He et al., 2013). Additionally, Reichstein et al. (2014) showed that the functional biogeographical variations of ecosystem properties were only partially explained by climate and PFTs. The large variability of biogeochemical processes within each PFT (Kattge et al., 2011) depended even more on plant traits, such as allocation and stabilization of carbon in the soil. Future studies should explicitly include the site-level information and trait database to test the relation between ecosystem functions and organismic traits to accurately quantify carbon fluxes.

Finally, the simplistic aggregation of CO_2 hour by hour into 8-day averages may bias our quantification without considering the influence of the planetary boundary layer (PBL) development. The PBL depth and turbulence intensity have a strong impact on the vertical and horizontal distribution of CO_2 in the atmosphere (Yi et al., 2001). The covariance between surface fluxes of CO_2 and the atmospheric mixing process has a strong seasonal character (Helliker et al., 2004). Since the rectifier effect influences the horizontal and vertical distributions of CO_2 in the atmosphere, it can bias carbon flux quantification (Denning et al., 1995). We further noted that we have not explicitly differentiated CO_2 fertilization effects and its indirect effects on CO_2 uptake through affecting stomata openness

in these ANN simulations. Process-based ecosystem models shall incorporate both fertilization and indirect effects into regional GPP and NEE quantification.

5. Conclusion

When scaling site-level eddy flux data to a region, the atmospheric CO_2 concentration on GPP and NEE has rarely been incorporated. Here we made a step forward by considering this effect in quantifying regional GPP and NEE in the conterminous US. We constructed two sets of artificial neural networks incorporating remote sensing variables to upscale the AmeriFlux site-level data to the region for seven ecosystem types: one that incorporated CO_2 and a second that did not. Our results showed that both sets of models showed good performance and were able to capture the GPP and NEE variation when compared with previous published results and MODIS products. However, the GPP and NEE difference between two models exhibited a great spatial and seasonal variability, which was closely related with climate drivers (air temperature and vapor pressure deficit). In addition, the simulation without considering CO_2 effects fails to detect the ecosystem response to droughts in the southeastern US in 2006, indicating that drought-induced surface CO_2variation could have more constraint on the regional GPP and NEE qualification. This study is among the first to explore the CO_2 influence on the regional GPP and NEE estimation in upscaling eddy flux data to regional scales. Our study suggests that the spatially and temporally varied CO_2 concentration should be factored into GPP and NEE quantification when scaling eddy flux data to a region.

Acknowledgement

This study is supported through projects funded to Q. Z. by the NASA Land-Use and Land-Cover Change program (NASA-NNX09AI26G), Department of Energy (DE-FG02-08ER64599), the NSF Division of Information and Intelligent Systems (NSF-1028291), and the NSF Carbon and Water in the Earth Program (NSF-0630319). The supercomputing resource is provided by the Rosen Center for Advanced Computing at Purdue University. Special thanks to all scientists and supporting staffs at AmeriFlux sites. Finally, we acknowledged two anonymous reviewers for their comments. Gabriela Shirkey helped editing of the manuscript.

Appendix A. Supplementary data

Supplementary material related to this article can be found, in the online version, at http://dx.doi.org/10.1016/j.agrformet.2016.01.007.

References

Ainsworth, E.A., Long, S.P., 2005. What have we learned from 15 years of free-air CO_2 enrichment (FACE)? A meta-analytic review of the responses of photosynthesis, canopy properties and plant production to rising CO_2. New Phytol. 165, 351–372.

Ainsworth, E.A., Rogers, A., 2007. The response of photosynthesis and stomatal conductance to rising CO_2: mechanisms and environmental interactions. Plant. Cell Environ. 30, 258–270.

Alton, P.B., 2011. How useful are plant functional types in global simulations of the carbon, water, and energy cycles? J. Geophys. Res. 116, G01030, http://dx.doi.org/10.1029/2010JG001430.

Anderson, L.O., Malhi, Y., Aragão, L.E.O.C., Ladle, R., Arai, E., Barbier, N., Phillips, O., 2010. Remote sensing detection of droughts in Amazonian forest canopies. New Phytol. 187, 733–750.

Andrews, A.E., Kofler, J.D., Trudeau, M.E., Williams, J.C., Neff, D.H., Masarie, K.A., Chao, D.Y., Kitzis, D.R., Novelli, P.C., Zhao, C.L., Dlugokencky, E.J., Lang, P.M., Crotwell, M.J., Fischer, M.L., Parker, M.J., Lee, J.T., Baumann, D.D., Desai, A.R., Stanier, C.O., De Wekker, S.F.J., Wolfe, D.E., Munger, J.W., Tans, P.P., 2014. CO_2, CO, and CH_4 measurements from tall towers in the NOAA Earth System Research Laboratory's Global Greenhouse Gas Reference Network: instrumentation, uncertainty analysis, and recommendations for future high-accuracy greenhouse gas monitoring efforts. Atmos. Meas. Tech. 7, 647–687, http://dx.doi.org/10.5194/amt-7-647-2014.

Aubinet, M., Grelle, A., Ibrom, A., Rannik, Ü., Moncrieff, J., Foken, T., Kowalski, A.S., Martin, P.H., Berbigier, P., Bernhofer, C., 1999. Estimates of the annual net carbon and water exchange of forests: the EUROFLUX methodology. Adv. Ecol. Res. 30, 113–175.

Baldocchi, D.D., 1997. Measuring and modelling carbon dioxide and water vapour exchange over a temperate broad-leaved forest during the 1995 summer drought. Plant. Cell Environ. 20, 1108–1122.

Baldocchi, D.D., 2008. TURNER REVIEW No. 15.'Breathing'of the terrestrial biosphere: lessons learned from a global network of carbon dioxide flux measurement systems. Aust. J. Bot. 56, 1–26.

Baldocchi, D.D., Falge, E., Gu, L., Olson, R., Hollinger, D., Running, S., Anthoni, P., Bernhofer, C., Davis, K., Evans, R., 2001. FLUXNET: a new tool to study the temporal and spatial variability of ecosystem-scale carbon dioxide, water vapor, and energy flux densities. Bull. Am. Meteorol. Soc. 82, 2415–2434.

Baldocchi, D.D., Hicks, B.B., Meyers, T.P., 1988. Measuring biosphere-atmosphere exchanges of biologically related gases with micrometeorological methods. Ecology 69, 1331–1340.

Beer, C., Reichstein, M., Tomelleri, E., Ciais, P., Jung, M., Carvalhais, N., Rödenbeck, C., Arain, M.A., Baldocchi, D., Bonan, G.B., 2010. Terrestrial gross carbon dioxide uptake: global distribution and covariation with climate. Science 329, 834–838.

Birdsey, R.A., Lewis, G.M., 2003. Current and Historical Trends in Use, Management, and Disturbance of US Forestlands. CRC Press, Baton Rouge, FL, pp. 15–34.

Bonan, G.B., 2008. Forests and climate change: forcings, feedbacks, and the climate benefits of forests. Science 320, 1444–1449.

Bracho, R., Starr, G., Gholz, H.L., Martin, T.A., Cropper, W.P., Loescher, H.W., 2012. Controls on carbon dynamics by ecosystem structure and climate for southeastern US slash pine plantations. Ecol. Monogr. 82, 101–128.

Bunce, J.A., 2004. Carbon dioxide effects on stomatal responses to the environment and water use by crops under field conditions. Oecologia 140, 1–10.

Canadell, J.G., Le Quéré, C., Raupach, M.R., Field, C.B., Buitenhuis, E.T., Ciais, P., Conway, T.J., Gillett, N.P., Houghton, R.A., Marland, G., 2007. Contributions to accelerating atmospheric CO_2 growth from economic activity, carbon intensity, and efficiency of natural sinks. Proc. Natl. Acad. Sci. U.S.A. 104, 18866–18870.

Chen, M., Zhuang, Q., Cook, D.R., Coulter, R., Pekour, M., Scott, R.L., Munger, J.W., Bible, K., 2011. Quantification of terrestrial ecosystem carbon dynamics in the conterminous United States combining a process-based biogeochemical model and MODIS and AmeriFlux data. Biogeosci. Discuss. 8, 2721.

Conley, M.M., Kimball, B.A., Brooks, T.J., Pinter, P.J., Hunsaker, D.J., Wall, G.W., Adam, N.R., LaMorte, R.L., Matthias, A.D., Thompson, T.L., 2001. CO_2 enrichment increases water-use efficiency in sorghum. New Phytol. 151, 407–412.

Curtis, P.S., Wang, X., 1998. A meta-analysis of elevated CO_2 effects on woody plant mass, form, and physiology. Oecologia 113, 299–313.

Dai, A., 2013. Increasing drought under global warming in observations and models. Nat. Clim. Change 3, 52–58.

Davis, K.J., Bakwin, P.S., Yi, C., Berger, B.W., Zhao, C., Teclaw, R.M., Isebrands, J.G., 2003. The annual cycles of CO_2 and H_2O exchange over a northern mixed forest as observed from a very tall tower. Glob. Change Biol. 9, 1278–1293, http://dx.doi.org/10.1046/j.1365-2486.2003.00672.x.

Deng, Q., Zhou, G., Liu, J., Liu, S., Duan, H., Zhang, D., 2010. Responses of soil respiration to elevated carbon dioxide and nitrogen addition in young subtropical forest ecosystems in China. Biogeosciences 7, 315–328.

Deng, X., Joly, R.J., Hahn, D.T., 1990. The influence of plant water deficit on photosynthesis and translocation of 14C-labeled assimilates in cacao seedlings. Physiol. Plant. 78, 623–627.

Deng, F., Chen, J.M., Pan, Y., Peters, W., Birdsey, R., McCullough, K., Xiao, J., 2013. The use of forest stand age information in an atmospheric CO_2 inversion applied to North America. Biogeosciences 10, 5335–5348, http://dx.doi.org/10.5194/bg-10-5335-2013.

Denning, A.S., Fung, I.Y., Randall, D., 1995. Latitudinal gradient of atmospheric CO_2 due to seasonal exchange with land biota. Nature 376, 240–243.

Dermody, O., Weltzin, J.F., Engel, E.C., Allen, P., Norby, R.J., 2007. How do elevated CO_2, warming, and reduced precipitation interact to affect soil moisture and LAI in an old field ecosystem? Plant Soil 301, 255–266.

Desai, A.R., Richardson, A.D., Moffat, A.M., Kattge, J., Hollinger, D.Y., Barr, A., Falge, E., Noormets, A., Papale, D., Reichstein, M., 2008. Cross-site evaluation of eddy covariance GPP and RE decomposition techniques. Agric. For. Meteorol. 148, 821–838.

Dijkstra, F.A., Blumenthal, D., Morgan, J.A., Pendall, E., Carrillo, Y., Follett, R.F., 2010. Contrasting effects of elevated CO_2 and warming on nitrogen cycling in a semiarid grassland. New Phytol. 187, 426–437.

Drake, B.G., Gonzàlez-Meler, M.A., Long, S.P., 1997. More efficient plants: a consequence of rising atmospheric CO_2? Annu. Rev. Plant Biol. 48, 609–639.

Eby, M., Zickfeld, K., Montenegro, A., Archer, D., Meissner, K.J., Weaver, A.J., 2009. Lifetime of anthropogenic climate change: millennial time scales of potential CO_2 and surface temperature perturbations. J. Clim. 22, 2501–2511.

Emmett, B.A., Beier, C., Estiarte, M., Tietema, A., Kristensen, H.L., Williams, D., Penuelas, J., Schmidt, I., Sowerby, A., 2004. The response of soil processes to climate change: results from manipulation studies of shrublands across an environmental gradient. Ecosystems 7, 625–637.

Farquhar, G.D., von Caemmerer, S., Berry, J.A., 1980. A biochemical model of photosynthetic CO_2 assimilation in leaves of C3 species. Planta 149, 78–90.

Foken, T., Wichura, B., 1996. Tools for quality assessment of surface-based flux measurements. Agric. For. Meteorol. 78, 83–105.

Fu, D., Chen, B., Zhang, H., Wang, J., Black, T.A., Amiro, B., Bohrer, G., Bolstad, P., Coulter, R., Rahman, F., 2014. Estimating landscape net ecosystem exchange at high spatial–temporal resolution based on Landsat data, an improved

upscaling model framework, and eddy covariance flux measurements. Remote Sens. Environ. 141, 90–104.
Geels, C., Gloor, M., Ciais, P., Bousquet, P., Peylin, P., Vermeulen, A.T., Dargaville, R., Aalto, T., Brandt, J., Christensen, J.H., Frohn, L.M., Haszpra, L., Karstens, U., Rödenbeck, C., Ramonet, M., Carboni, G., Santaguida, R., 2007. Comparing atmospheric transport models for future regional inversions over Europe; Part 1: Mapping the atmospheric CO_2 signals. Atmos. Chem. Phys. 7, 3461–3479, http://dx.doi.org/10.5194/acp-7-3461-2007.
Gill, R.A., Polley, H.W., Johnson, H.B., Anderson, L.J., Maherali, H., Jackson, R.B., 2002. Nonlinear grassland responses to past and future atmospheric CO_2. Nature 417, 279–282.
Gu, Y., Brown, J.F., Verdin, J.P., Wardlow, B., 2007. A five-year analysis of MODIS NDVI and NDWI for grassland drought assessment over the central Great Plains of the United States. Geophys. Res. Lett. 34, L06407, http://dx.doi.org/10.1029/2006GL029127.
Gu, Y., Hunt, E., Wardlow, B., Basara, J.B., Brown, J.F., Verdin, J.P., 2008. Evaluation of MODIS NDVI and NDWI for vegetation drought monitoring using Oklahoma Mesonet soil moisture data. Geophys. Res. Lett. 35, L22401, http://dx.doi.org/10.1029/2008GL035772.
Hanan, N.P., Burba, G., Verma, S.B., Berry, J.A., Suyker, A., Walter-Shea, E.A., 2002. Inversion of net ecosystem CO_2 flux measurements for estimation of canopy PAR absorption. Glob. Chang. Biol. 8, 563–574, http://dx.doi.org/10.1046/j.1365-2486.2002.00488.x.
Hanson, P.J., Amthor, J.S., Wullschleger, S.D., Wilson, K.B., Grant, R.F., Hartley, A., Hui, D., Hunt, E., Raymond, J., Johnson, D.W., Kimball, J.S., 2004. Oak forest carbon and water simulations: model intercomparisons and evaluations against independent data. Ecol. Monogr. 74, 443–489.
Hargrove, W.W., Hoffman, F.M., Law, B.E., 2003. New analysis reveals representativeness of the AmeriFlux network. Eos Trans. Am. Geophys. Union 84, 529–535.
Hartmann, J., West, A.J., Renforth, P., Köhler, P., De La Rocha, C.L., Wolf-Gladrow, D.A., Dürr, H.H., Scheffran, J., 2013. Enhanced chemical weathering as a geoengineering strategy to reduce atmospheric carbon dioxide, supply nutrients, and mitigate ocean acidification. Rev. Geophys. 51, 113–149.
Haszpra, L., Barcza, Z., Hidy, D., Szilágyi, I., Dlugokencky, E., Tans, P., 2008. Trends and temporal variations of major greenhouse gases at a rural site in Central Europe. Atmos. Environ. 42, 8707–8716, http://dx.doi.org/10.1016/j.atmosenv.2008.09.012.
He, Y., Zhuang, Q., David McGuire, A., Liu, Y., Chen, M., 2013. Alternative ways of using field-based estimates to calibrate ecosystem models and their implications for carbon cycle studies. J. Geophys. Res. Biogeosci. 118, 983–993, http://dx.doi.org/10.1002/jgrg.20080.
Helliker, B.R., Berry, J.A., Betts, A.K., Bakwin, P.S., Davis, K.J., Denning, A.S., Ehleringer, J.R., Miller, J.B., Butler, M.P., Ricciuto, D.M., 2004. Estimates of net CO_2 flux by application of equilibrium boundary layer concepts to CO_2 and water vapor measurements from a tall tower. J. Geophys. Res. Atmos. 109, D20106, http://dx.doi.org/10.1029/2004JD004532.
Hirata, R., Saigusa, N., Yamamoto, S., Ohtani, Y., Ide, R., Asanuma, J., Gamo, M., Hirano, T., Kondo, H., Kosugi, Y., 2008. Spatial distribution of carbon balance in forest ecosystems across East Asia. Agric. For. Meteorol. 148, 761–775.
Hovenden, M.J., Newton, P.C.D., Carran, R.A., Theobald, P., Wills, K.E., Vander Schoor, J.K., Williams, A.L., Osanai, Y., 2008. Warming prevents the elevated CO_2-induced reduction in available soil nitrogen in a temperate, perennial grassland. Glob. Chang. Biol. 14, 1018–1024.
Huete, A., Didan, K., Miura, T., Rodriguez, E.P., Gao, X., Ferreira, L.G., 2002. Overview of the radiometric and biophysical performance of the MODIS vegetation indices. Remote Sens. Environ. 83, 195–213.
Janssens, I.A., Freibauer, A., Ciais, P., Smith, P., Nabuurs, G.-J., Folberth, G., Schlamadinger, B., Hutjes, R.W.A., Ceulemans, R., Schulze, E.-D., 2003. Europe's terrestrial biosphere absorbs 7 to 12% of European anthropogenic CO_2 emissions. Science 300, 1538–1542.
Jung, M., Verstraete, M., Gobron, N., Reichstein, M., Papale, D., Bondeau, A., Robustelli, M., Pinty, B., 2008. Diagnostic assessment of European gross primary production. Glob. Change Biol. 14, 2349–2364.
Kato, T., Tang, Y., 2008. Spatial variability and major controlling factors of CO_2 sink strength in Asian terrestrial ecosystems: evidence from eddy covariance data. Glob. Change Biol. 14, 2333–2348.
Kattge, J., Diaz, S., Lavorel, S., Prentice, I.C., Leadley, P., et al., 2011. TRY—a global database of plant traits. Glob. Change Biol. 17, 2905–2935.
Keeling, C.D., Whorf, T.P., Wahlen, M., van der, Plicht J., 1995. Interannual extremes in the rate of rise of atmospheric carbon dioxide since 1980. Nature 375, 666–670.
Keenan, T.F., Hollinger, D.Y., Bohrer, G., Dragoni, D., Munger, J.W., Schmid, H.P., Richardson, A.D., 2013. Increase in forest water-use efficiency as atmospheric carbon dioxide concentrations rise. Nature 499, 324–327.
Keppel-Aleks, G., Wolf, A.S., Mu, M., Doney, S.C., Morton, D.C., Kasibhatla, P.S., Miller, J.B., Dlugokencky, E.J., Randerson, J.T., 2014. Separating the influence of temperature, drought, and fire on interannual variability in atmospheric CO_2. Glob. Biogeochem. Cycles 28, 1295–1310, http://dx.doi.org/10.1002/2014GB004890.
Kirschbaum, M.U.F., King, D.A., Comins, H.N., McMurtrie, R.E., Medlyn, B.E., Pongracic, S., Murty, D., Keith, H., Raison, R.J., Khanna, P.K., 1994. Modelling forest response to increasing CO_2 concentration under nutrient-limited conditions. Plant. Cell Environ. 17, 1081–1099.
Knorr, W., Scholze, M., Gobron, N., Pinty, B., Kaminski, T., 2005. Global-scale drought caused atmospheric CO_2 increase. Eos Trans. Am. Geophys. Union 86, 178–181.
Lambers, H., Chapin III, F.S., Pons, T.L., 2008. Plant Water Relations. Springer, New York, USA, pp. 163–223.
Lambin, E.F., Geist, H.J., Lepers, E., 2003. Dynamics of land-use and land-cover change in tropical regions. Annu. Rev. Environ. Resour. 28, 205–241.
Larsen, K.S., Andresen, L.C., Beier, C., Jonasson, S., Albert, K.R., Ambus, P.E.R., Arndal, M.F., Carter, M.S., Christensen, S., Holmstrup, M., 2011. Reduced N cycling in response to elevated CO_2, warming, and drought in a Danish heathland: synthesizing results of the CLIMAITE project after two years of treatments. Glob. Change Biol. 17, 1884–1899.
Lauvaux, T., Schuh, A.E., Bocquet, M., Wu, L., Richardson, S., Miles, N., Davis, K.J., 2012. Network design for mesoscale inversions of CO_2 sources and sinks. Tellus B 64, http://dx.doi.org/10.3402/tellusb.v64i0.17980.
Law, B.E., Anthoni, P.M., Aber, J.D., 2000. Measurements of gross and net ecosystem productivity and water vapour exchange of a Pinus ponderosa ecosystem, and an evaluation of two generalized models. Glob. Change Biol. 6, 155–168.
Law, B.E., Falge, E., Gu, L.V., Baldocchi, D.D., Bakwin, P., Berbigier, P., Davis, K., Dolman, A.J., Falk, M., Fuentes, J.D., 2002. Environmental controls over carbon dioxide and water vapor exchange of terrestrial vegetation. Agric. For. Meteorol. 113, 97–120.
Li, C., Wang, K., 2003. Differences in drought responses of three contrasting *Eucalyptus microtheca* F. Muell. Popul. For. Ecol. Manage. 179, 377–385.
Li, F.Y., Newton, P.C., Lieffering, M., 2014. Testing simulations of intra- and inter-annual variation in the plant production response to elevated CO_2 against measurements from an 11-year FACE experiment on grazed pasture. Glob. Change Biol. 20 (1), 228–239.
Lloyd, J., Taylor, J.A., 1994. On the temperature dependence of soil respiration. Funct. Ecol. 8, 315–323, http://dx.doi.org/10.2307/2389824.
Loescher, H.W., Law, B.E., Mahrt, L., Hollinger, D.Y., Campbell, J., Wofsy, S.C., 2006. Uncertainties in, and interpretation of, carbon flux estimates using the eddy covariance technique. J. Geophys. Res. 111, D21S90, http://dx.doi.org/10.1029/2005JD006932.
Los, S.O., 2013. Analysis of trends in fused AVHRR and MODIS NDVI data for 1982-2006: indication for a CO_2 fertilization effect in global vegetation. Glob. Biogeochem. Cycles 27, 318–330.
Lund, M., Lafleur, P.M., Roulet, N.T., Lindroth, A., Christensen, T.R., Aurela, M., Chojnicki, B.H., Flanagan, L.B., Humphreys, E.R., Laurila, T., 2010. Variability in exchange of CO_2 across 12 northern peatland and tundra sites. Glob. Change Biol. 16, 2436–2448.
Luo, Y., Jackson, R.B., Field, C.B., Mooney, H.A., 1996. Elevated CO_2 increases belowground respiration in California grasslands. Oecologia 108, 130–137.
Luo, Y., Su, B.O., Currie, W.S., Dukes, J.S., Finzi, A., Hartwig, U., Hungate, B., McMurtrie, R.E., Oren, R.A.M., Parton, W.J., 2004. Progressive nitrogen limitation of ecosystem responses to rising atmospheric carbon dioxide. Bioscience 54, 731–739.
Madani, N., Kimball, J.S., Affleck, D.L.R., Kattge, J., Graham, J., Bodegom, P.M., Reich, P.B., Running, S.W., 2014. Improving ecosystem productivity modeling through spatially explicit estimation of optimal light use efficiency. J. Geophys. Res. Biogeosci. 119, 1755–1769.
Masarie, K.A., Pétron, G., Andrews, A., Bruhwiler, L., Conway, T.J., Jacobson, A.R., Miller, J.B., Tans, P.P., Worthy, D.E., Peters, W., 2011. Impact of CO_2 measurement bias on CarbonTracker surface flux estimates. J. Geophys. Res. 116, D17305, http://dx.doi.org/10.1029/2011JD016270.
Medlyn, B.E., Barton, C.V.M., Broadmeadow, M.S.J., Ceulemans, R., De Angelis, P., Forstreuter, M., Freeman, M., Jackson, S.B., Kellomaki, S., Laitat, E., Rey, A., Roberntz, P., Sigurdsson, B.D., Strassemeyer, J., Wang, K., Curtis, P.S., Jarvis, P.G., 2001. Stomatal conductance of forest species after long-term exposure to elevated CO_2 concentration: a synthesis. New Phytol. 149, 247–264, http://dx.doi.org/10.1046/j.1469-8137.2001.00028.x.
Melton, J.R., Arora, V.K., 2013. Sub-grid scale representation of vegetation in global land surface schemes: implications for estimation of the terrestrial carbon sink. Biogeosci. Discuss. 10, 16003–16041.
Mesinger, F., DiMego, G., Kalnay, E., Mitchell, K., Shafran, P.C., Ebisuzaki, W., Jovic, D., Woollen, J., Rogers, E., Berbery, E.H., 2006. North American regional reanalysis. Bull. Am. Meteorol. Soc. 87, 343–360.
Miles, N.L., Richardson, S.J., Davis, K.J., Lauvaux, T., Andrews, A.E., West, T.O., Bandaru, V., Crosson, E.R., 2012. Large amplitude spatial and temporal gradients in atmospheric boundary layer CO_2 mole fractions detected with a tower-based network in the U.S. upper Midwest. J. Geophys. Res. Biogeosci. 117, G01019, http://dx.doi.org/10.1029/2011JG001781.
Moffat, A.M., Papale, D., Reichstein, M., Hollinger, D.Y., Richardson, A.D., Barr, A.G., Beckstein, C., Braswell, B.H., Churkina, G., Desai, A.R., 2007. Comprehensive comparison of gap-filling techniques for eddy covariance net carbon fluxes. Agric. For. Meteorol. 147, 209–232.
Morgan, J.A., Pataki, D.E., Körner, C., Clark, H., Del Grosso, S.J., Grünzweig, J.M., Knapp, A.K., Mosier, A.R., Newton, P.C.D., Niklaus, P.A., 2004. Water relations in grassland and desert ecosystems exposed to elevated atmospheric CO_2. Oecologia 140, 11–25.
Myneni, R.B., Hoffman, S., Knyazikhin, Y., Privette, J.L., Glassy, J., Tian, Y., Wang, Y., Song, X., Zhang, Y., Smith, G.R., 2002. Global products of vegetation leaf area and fraction absorbed PAR from year one of MODIS data. Remote Sens. Environ. 83, 214–231.

Norby, R.J., Warren, J.M., Iversen, C.M., Medlyn, B.E., McMurtrie, R.E., 2010. CO_2 enhancement of forest productivity constrained by limited nitrogen availability. Proc. Natl. Acad. Sci. U.S.A. 107, 19368–19373.
Nowak, R.S., Ellsworth, D.S., Smith, S.D., 2004. Functional responses of plants to elevated atmospheric CO_2—do photosynthetic and productivity data from FACE experiments support early predictions? New Phytol. 162, 253–280.
Oren, R., Ellsworth, D.S., Johnsen, K.H., Phillips, N., Ewers, B.E., Maier, C., Schäfer, K.V.R., McCarthy, H., Hendrey, G., McNulty, S.G., 2001. Soil fertility limits carbon sequestration by forest ecosystems in a CO_2-enriched atmosphere. Nature 411, 469–472.
Pan, Y., Chen, J.M., Birdsey, R., McCullough, K., He, L., Deng, F., 2011. Age structure and disturbance legacy of North American forests. Biogeosciences 8, 715–732, http://dx.doi.org/10.5194/bg-8-715-2011.
Park, S., Feddema, J.J., Egbert, S.L., 2004. Impacts of hydrologic soil properties on drought detection with MODIS thermal data. Remote Sens. Environ. 89, 53–62.
Peltola, H., Kilpeläinen, A., Kellomäki, S., 2002. Diameter growth of Scots pine (*Pinus sylvestris*) trees grown at elevated temperature and carbon dioxide concentration under boreal conditions. Tree Physiol. 22, 963–972.
Peters, W., Jacobson, A.R., Sweeney, C., Andrews, A.E., Conway, T.J., Masarie, K., Miller, J.B., Bruhwiler, L.M.P., Petron, G., Hirsch, A.I., 2007. An atmospheric perspective on North American carbon dioxide exchange: CarbonTracker. Proc. Natl. Acad. Sci. U.S.A. 104, 18925–18930.
Piao, S., Friedlingstein, P., Ciais, P., Zhou, L., Chen, A., 2006. Effect of climate and CO_2 changes on the greening of the Northern Hemisphere over the past two decades. Geophys. Res. Lett. 33, L23402, http://dx.doi.org/10.1029/2006GL028205.
Prince, S.D., Goward, S.N., 1995. Global primary production: a remote sensing approach. J. Biogeogr. 22, 815–835.
Rahman, A.F., Sims, D.A., Cordova, V.D., El-Masri, B.Z., 2005. Potential of MODIS EVI and surface temperature for directly estimating per-pixel ecosystem C fluxes. Geophys. Res. Lett. 32, L19404, http://dx.doi.org/10.1029/2005GL024127.
Raich, J.W., Rastetter, E.B., Melillo, J.M., Kicklighter, D.W., Steudler, P.A., Peterson, B.J., Grace, A.L., Moore Iii, B., Vörösmarty, C.J., 1991. Potential net primary productivity in South America: application of a global model. Ecol. Appl. 1, 399–429.
Raich, J.W., Schlesinger, W.H., 1992. The global carbon dioxide flux in soil respiration and its relationship to vegetation and climate. Tellus B 44, 81–99, http://dx.doi.org/10.1034/j.1600-0889.1992.t01-1-00001.x.
Reich, P.B., Wright, I.J., Lusk, C.H., 2007. Predicting leaf physiology from simple plant and climate attributes: a global GLOPNET analysis. Ecol. Appl. 17, 1982–1988, http://dx.doi.org/10.1890/06-1803.1.
Reich, P.B., Hobbie, S.E., Lee, T.D., 2014. Plant growth enhancement by elevated CO_2 eliminated by joint water and nitrogen limitation. Nat. Geosci. 7, 920–924.
Reichstein, M., Tenhunen, J.D., Roupsard, O., Ourcival, J., Rambal, S., Miglietta, F., Peressotti, A., Pecchiari, M., Tirone, G., Valentini, R., 2002. Severe drought effects on ecosystem CO_2 and H_2O fluxes at three Mediterranean evergreen sites: revision of current hypotheses? Glob. Change Biol. 8, 999–1017.
Reichstein, M., Bahn, M., Mahecha, M.D., Kattge, J., Baldocchi, D.D., 2014. Linking plant and ecosystem functional biogeography. Proc. Natl. Acad. Sci. U.S.A. 111, 13697–13702, http://dx.doi.org/10.1073/pnas.1216065111.
Ruehr, N.K., Offermann, C.A., Gessler, A., Winkler, J.B., Ferrio, J.P., Buchmann, N., Barnard, R.L., 2009. Drought effects on allocation of recent carbon: from beech leaves to soil CO_2 efflux. New Phytol. 184, 950–961.
Running, S.W., Thornton, P.E., Nemani, R., Glassy, J.M., 2000. Global terrestrial gross and net primary productivity from the earth observing system. In: Methods in Ecosystem Science. Springer, New York, USA, pp. 44–57.
Running, S.W., Nemani, R.R., Heinsch, F.A., Zhao, M., Reeves, M., Hashimoto, H., 2004. A continuous satellite-derived measure of global terrestrial primary production. Bioscience 54, 547–560.
Schwarz, P.A., Law, B.E., Williams, M., Irvine, J., Kurpius, M., Moore, D., 2004. Climatic versus biotic constraints on carbon and water fluxes in seasonally drought-affected ponderosa pine ecosystems. Glob. Biogeochem. Cycles 18 (18), GB4007, http://dx.doi.org/10.1029/2004GB002234.
Singh, R.P., Roy, S., Kogan, F., 2003. Vegetation and temperature condition indices from NOAA AVHRR data for drought monitoring over India. Int. J. Remote Sens. 24, 4393–4402.
Son, N.T., Chen, C.F., Chen, C.R., Chang, L.Y., Minh, V.Q., 2012. Monitoring agricultural drought in the Lower Mekong Basin using MODIS NDVI and land surface temperature data. Int. J. Appl. Earth Obs. Geoinf. 18, 417–427.
Song, X., Saito, G., Kodama, M., Sawada, H., 2004. Early detection system of drought in East Asia using NDVI from NOAA/AVHRR data. Int. J. Remote Sens. 25, 3105–3111.
Sowerby, A., Emmett, B.A., Tietema, A., Beier, C., 2008. Contrasting effects of repeated summer drought on soil carbon efflux in hydric and mesic heathland soils. Glob. Change Biol. 14, 2388–2404.
Specht, D.F., 1991. A general regression neural network. IEEE Trans. Neural Networks 2, 568–576.
Tans, P.P., Fung, I.Y., Takahashi, T., 1990. Observational contrains on the global atmospheric CO_2 budget. Science 247, 1431–1438.
Tingey, D.T., Mckane, R.B., Olszyk, D.M., Johnson, M.G., Rygiewicz, P.T., Henry Lee, E., 2003. Elevated CO_2 and temperature alter nitrogen allocation in Douglas-fir. Glob. Change Biol. 9, 1038–1050.
Tucker, C.J., 1979. Red and photographic infrared linear combinations for monitoring vegetation. Remote Sens. Environ. 8, 127–150.
Turner, D.P., Ritts, W.D., Cohen, W.B., Gower, S.T., Zhao, M., Running, S.W., Wofsy, S.C., Urbanski, S., Dunn, A.L., Munger, J.W., 2003. Scaling gross primary production (GPP) over boreal and deciduous forest landscapes in support of MODIS GPP product validation. Remote Sens. Environ. 88, 256–270.
Turner, D.P., Ritts, W.D., Cohen, W.B., Gower, S.T., Running, S.W., Zhao, M., Costa, M.H., Kirschbaum, A.A., Ham, J.M., Saleska, S.R., Ahl, D.E., 2006. Evaluation of MODIS NPP and GPP products across multiple biomes. Remote Sens. Environ. 102, 282–292, http://dx.doi.org/10.1016/j.rse.2006.02.017.
Valentini, R., Matteucci, G., Dolman, A.J., Schulze, E.-D., Rebmann, C., Moors, E.J., Granier, A., Gross, P., Jensen, N.O., Pilegaard, K., 2000. Respiration as the main determinant of carbon balance in European forests. Nature 404, 861–865.
Vetter, M., Churkina, G., Jung, M., Reichstein, M., Zaehle, S., Bondeau, A., Chen, Y., Ciais, P., Feser, F., Freibauer, A., 2008. Analyzing the causes and spatial pattern of the European 2003 carbon flux anomaly using seven models. Biogeosciences 5, 561–583.
Wall, G.W., Brooks, T.J., Adam, N.R., Cousins, A.B., Kimball, B.A., Pinter, P.J., LaMorte, R.L., Triggs, J., Ottman, M.J., Leavitt, S.W., 2001. Elevated atmospheric CO_2 improved sorghum plant water status by ameliorating the adverse effects of drought. New Phytol. 152, 231–248.
Wan, S., Norby, R.J., Ledford, J., Weltzin, J.F., 2007. Responses of soil respiration to elevated CO_2, air warming, and changing soil water availability in a model old-field grassland. Glob. Change Biol. 13, 2411–2424.
Wan, Z., Zhang, Y., Zhang, Q., Li, Z., 2002. Validation of the land-surface temperature products retrieved from Terra Moderate Resolution Imaging Spectroradiometer data. Remote Sens. Environ. 83, 163–180.
Wan, Z., Wang, P., Li, X., 2004. Using MODIS land surface temperature and normalized difference vegetation index products for monitoring drought in the southern Great Plains, USA. Int. J. Remote Sens. 25, 61–72.
White, M.A., Thornton, P.E., Running, S.W., Nemani, R.R., 2000. Parameterization and sensitivity analysis of the BIOME-BGC terrestrial ecosystem model: net primary production controls. Earth Interact. 4, 1–85.
Xiao, J., Zhuang, Q., Baldocchi, D.D., Law, B.E., Richardson, A.D., Chen, J., Oren, R., Starr, G., Noormets, A., Ma, S., Verma, S.B., Wharton, S., Wofsy, S.C., Bolstad, P.V., Burns, S.P., Cook, D.R., Curtis, P.S., Drake, B.G., Falk, M., Fischer, M.L., Foster, D.R., Gu, L., Hadley, J.L., Hollinger, D.Y., Katul, G.G., Litvak, M., Martin, T.A., Matamala, R., McNulty, S., Meyers, T.P., Monson, R.K., Munger, J.W., Oechel, W.C., Paw, U.K.T., Schmid, H.P., Scott, R.L., Sun, G., Suyker, A.E., Torn, M.S., 2008. Estimation of net ecosystem carbon exchange for the conterminous United States by combining MODIS and AmeriFlux data. Agric. For. Meteorol. 148, 1827–1847, http://dx.doi.org/10.1016/j.agrformet.2008.06.015.
Xiao, J.F., Zhuang, Q.L., Law, B.E., Chen, J.Q., Baldocchi, D.D., Cook, D.R., Oren, R., Richardson, A.D., Wharton, S., Ma, S.Y., Martini, T.A., Verma, S.B., Suyker, A.E., Scott, R.L., Monson, R.K., Litvak, M., Hollinger, D.Y., Sun, G., Davis, K.J., Bolstad, P.V., Burns, S.P., Curtis, P.S., Drake, B.G., Falk, M., Fischer, M.L., Foster, D.R., Gu, L.H., Hadley, J.L., Katul, G.G., Roser, Y., McNulty, S., Meyers, T.P., Munger, J.W., Noormets, A., Oechel, W.C., Paw, K.T., Schmid, H.P., Starr, G., Torn, M.S., Wofsy, S.C., 2010. A continuous measure of gross primary production for the conterminous United States derived from MODIS and AmeriFlux data. Remote Sens. Environ. 114, 576–591.
Xiao, J., Chen, J., Davis, K.J., Reichstein, M., 2012. Advances in upscaling of eddy covariance measurements of carbon and water fluxes. J. Geophys. Res. Biogeosci. 117, G00J01, http://dx.doi.org/10.1029/2011JG001889.
Xiao, J., Ollinger, S.V., Frolking, S., Hurtt, G.C., Hollinger, D.Y., Davis, K.J., Pan, Y., Zhang, X., Deng, F., Chen, J., Baldocchi, D.D., Law, B.E., Arain, M.A., Desai, A.R., Richardson, A.D., Sun, G., Amiro, B., Margolis, H., Gu, L., Scott, R.L., Blanken, P.D., Suyker, A.E., 2014. Data-driven diagnostics of terrestrial carbon dynamics over North America. Agric. For. Meteorol. 197, 142–157, http://dx.doi.org/10.1016/j.agrformet.2014.06.013.
Yang, F., Ichii, K., White, M.A., Hashimoto, H., Michaelis, A.R., Votava, P., Zhu, A., Huete, A., Running, S.W., Nemani, R.R., 2007. Developing a continental-scale measure of gross primary production by combining MODIS and AmeriFlux data through Support Vector Machine approach. Remote Sens. Environ. 110, 109–122.
Yi, C., Davis, K.J., Berger, B.W., Bakwin, P.S., 2001. Long-term observations of the dynamics of the continental planetary boundary layer. J. Atmos. Sci. 58, 1288–1299.
Yu, G., Zhu, X., Fu, Y., He, H., Wang, Q., Wen, X., Li, X., Zhang, L., Zhang, L., Su, W., 2013. Spatial patterns and climate drivers of carbon fluxes in terrestrial ecosystems of China. Glob. Change Biol. 19, 798–810.
Yuan, W., Liu, S., Yu, G., Bonnefond, J.-M., Chen, J., Davis, K., Desai, A.R., Goldstein, A.H., Gianelle, D., Rossi, F., 2010. Global estimates of evapotranspiration and gross primary production based on MODIS and global meteorology data. Remote Sens. Environ. 114, 1416–1431.
Zhu, X.-J., Yu, G.-R., He, H.-L., Wang, Q.-F., Chen, Z., Gao, Y.-N., Zhang, Y.-P., Zhang, J.-H., Yan, J.-H., Wang, H.-M., Zhou, G.-S., Jia, B.-R., Xiang, W.-H., Li, Y.-N., Zhao, L., Wang, Y.-F., Shi, P.-L., Chen, S.-P., Xin, X.-P., Zhao, F.-H., Wang, Y.-Y., Tong, C.-L., Fu, Y.-L., Wen, X.-F., Liu, Y.-C., Zhang, L.-M., Zhang, L., Su, W., Li, S.-G., Sun, X.-M., 2014. Geographical statistical assessments of carbon fluxes in terrestrial ecosystems of China: results from upscaling network observations. Glob. Planet. Change 118, 52–61, http://dx.doi.org/10.1016/j.gloplacha.2014.04.003.
Zhuang, Q., Lu, Y., Chen, M., 2012. An inventory of global N_2O emissions from the soils of natural terrestrial ecosystems. Atmos. Environ. 47, 66–75.